

A Surface Oxidised Fe-S catalyst for the Liquid Phase Hydrogenation of CO₂.

Claire E. Mitchell^a, Umberto Terranova^{a,b}, Andrew M. Beale^{c,d}, Wilm Jones^{c,d}, David J. Morgan^a, Meenakshisundaram Sankar^{a}, Nora H. de Leeuw^{a,e*}*

[a] Cardiff Catalysis Institute, School of Chemistry, Cardiff University, Cardiff, CF10 4AT, United Kingdom

[b] School of Postgraduate Medicine and Allied Health, Crewe campus, University of Buckingham, Crewe, CW1 5DU, United Kingdom

[c] Department of Chemistry, University College London, London, WC1H 0AJ, United Kingdom

[d] Research Complex at Harwell, Rutherford Appleton Laboratory, Harwell Science & Innovation Campus, Harwell, Didcot, OX11 0FA, United Kingdom

[e] School of Chemistry, University of Leeds, Leeds, LS2 9JT, United Kingdom

Correspondence to:

Dr. M. Sankar, Cardiff Catalysis Institute, School of Chemistry, Cardiff University, Cardiff, CF10 4AT, United Kingdom; Email: Sankar@cardiff.ac.uk

Prof. N. H. de Leeuw, School of Chemistry, University of Leeds, Leeds, LS2 9JT, United Kingdom; Email: n.h.deleeuw@leeds.ac.uk

Table of Contents

Methods.....	1
Catalyst Preparation	1
Catalytic CO ₂ Hydrogenation and product analyses	2
Catalyst Characterisation	3
Material Characterisation.....	4
<i>Figure S1</i>	4
<i>Table S1</i>	5
<i>Figure S2</i>	5
<i>Figure S3</i>	6
<i>Figure S4</i>	7
<i>Figure S5</i>	7
<i>Table S2</i>	8
<i>Figure S6</i>	9
Computational Details	10
Density Functional Theory Calculations	10
Computational Surface Models.....	11
<i>Figure S7</i>	11
<i>Figure S8</i>	12
<i>Figure S9</i>	12
References.....	13

Methods

Catalyst Preparation

The pyrrhotite synthesis was adapted from the procedure reported by Beal *et al.*¹ Iron(II) acetylacetonate, Fe(acac)₂ (99.9%) was obtained from Molekula. Sulfur (sublimed) (99.5%) (Alfa Aesar) and Oleylamine (OAm) (70%) (Sigma Aldrich). The synthesis was carried out in a three-necked flask equipped with a condenser, temperature probe and magnetic stirrer bar. OAm was initially degassed by bubbling nitrogen rapidly for 30 minutes, and the synthesis was done under nitrogen atmosphere. Fe(acac)₂ (1.155 g, 4.5 mmol) and sulfur (0.147 g, 4.5 mmol) were placed in a flask, and flushed with nitrogen. The degassed OAm (60 cm³) was added and stirred to produce a dark red suspension. While constantly bubbling nitrogen through the reaction mixture, the suspension was rapidly heated to the reaction temperature and held for a certain amount of time before being cooled to room temperature. The pyrrhotite synthesis were done at either 280°C or 310°C, and the synthesis time between 30 and 720 minutes. To remove the OAm, acetone was added (40cm³), followed by centrifugation and the organic brown supernatant layer was removed. To wash the black iron sulfide nanocrystals, the solid was then resuspended in toluene (Sigma Aldrich, 99.8%), followed by centrifugation. This step was repeated until the supernatant was clear and colourless. The sample was then left in a vacuum oven at room temperature overnight and stored as a powder in a sealed vial flushed with N₂.

Calcination of the power was performed in a furnace with air flowing at a specific temperature ranging from 150 – 700 °C, with a ramp rate of 5 °C/min. The calcination temperature was maintained for 4 hours. The material was cooled to room temperature before stored in a sealed vial flushed with N₂.

Catalytic CO₂ Hydrogenation and product analyses

The hydrogenation of CO₂ to formate was carried out in a high-pressure stainless steel 10 ml autoclave. In a typical reaction, 20mg of the catalyst was charged in a glass liner containing 4 ml of 1M NaOH and a stirrer bar, the glass liner was placed inside the autoclave reactor before the reactor was closed airtight. The reactor with its contents was first purged with N₂ (3 times) and then with CO₂ (3 times) to remove traces of air or oxygen from the system and then finally charged with 30 bar CO₂, the CO₂ was left to dissolve for 20 minutes at room temperature before the pressure was reduced to 10 bar, then H₂ (10 bar) was added. Then the reactor was heated to the reaction temperature (125 °C) while stirring at 1450 rpm. After 3 days of the reaction time the reactor was cooled to < 10 °C using an ice bath, the liquid sample was collected, and the solid catalyst was removed *via* centrifugation followed by filtration using a syringe filter fitted with a 45µl filter tip. The identity of the products (HCOOH) were confirmed and quantified using proton nuclear magnetic resonance (¹H-NMR) analysis (Bruker 500 MHz spectrometer), here 0.7ml of reaction solution was mixed with 0.1ml D₂O (for lock) and a sealed glass tube insert containing 1% tetramethylsilane (TMS) in CDCl₃ internal standard. The NMR was equipped with a solvent suppression system to suppress the water signal. A series of known standard solutions of formic acid were calibrated against the TMS insert generating a calibration curve and response factors which were used for quantitative analyses of the reaction mixtures.

Catalyst Characterisation

PXRD

The bulk structures were characterised using X-ray diffraction. Conventional powder X-ray diffraction (PXRD) analysis of the materials was performed on a (θ - θ) PANalytical X'pert Pro powder diffractometer with a Ni filtered CuK α radiation source operating at 40 keV and 40 mA. Patterns were recorded over the 2θ angular range 10-80° using a step size of 0.016°.

Raman

Raman spectroscopy was carried out using a Renishaw ramanoscope using spectrophysics 514 nm HeNe laser at a power of 10 mW. Spectra were obtained in the region of 100-1500 cm⁻¹.

TGA

Thermal gravimetric analysis (TGA) was performed using a Setaram Labsys 1600 instrument. Samples (5-10 mg) were loaded into alumina crucibles and heated to 900 °C (5 °C/min) in a flow of synthetic air (50 ml/min). For all specified TGA runs, blank runs were subtracted from the relevant data to remove buoyancy effects.

XPS

X-ray photoelectron spectroscopy (XPS) was performed on a Thermo Fisher Scientific K-alpha+ spectrometer. Samples were analysed using a micro-focused monochromatic Al x-ray source (72 W) over an elliptical area of approximately 400 μ m. Data were recorded at pass energies of 150 eV for survey scans and 40 eV for high resolution scan with 1 eV and 0.1 eV step sizes respectively. Charge neutralisation of the sample was achieved using a combination of both low energy electrons and argon ions. Data analysis was performed in CasaXPS using a Shirley type background and Scofield cross sections, with an energy dependence of -0.6.

XAFS

XAFS data was collected at the B18 beamline at the Diamond Light Source in Harwell, UK. The measurements were performed in transmission mode at Fe K edge. A Si(111) double crystal monochromator was used to select the energies. A Pt coated mirror was used to reject higher harmonics from the beam. The photon flux of the incoming and outgoing X-ray beam was detected with two ionization chambers I_0 and I_t , respectively, filled with appropriate mixtures of N_2/Ar . A third ionization chamber (I_{ref}) was used in series to simultaneously measure the corresponding reference metal foil. Data was processed using Athena software.

Material Characterisation

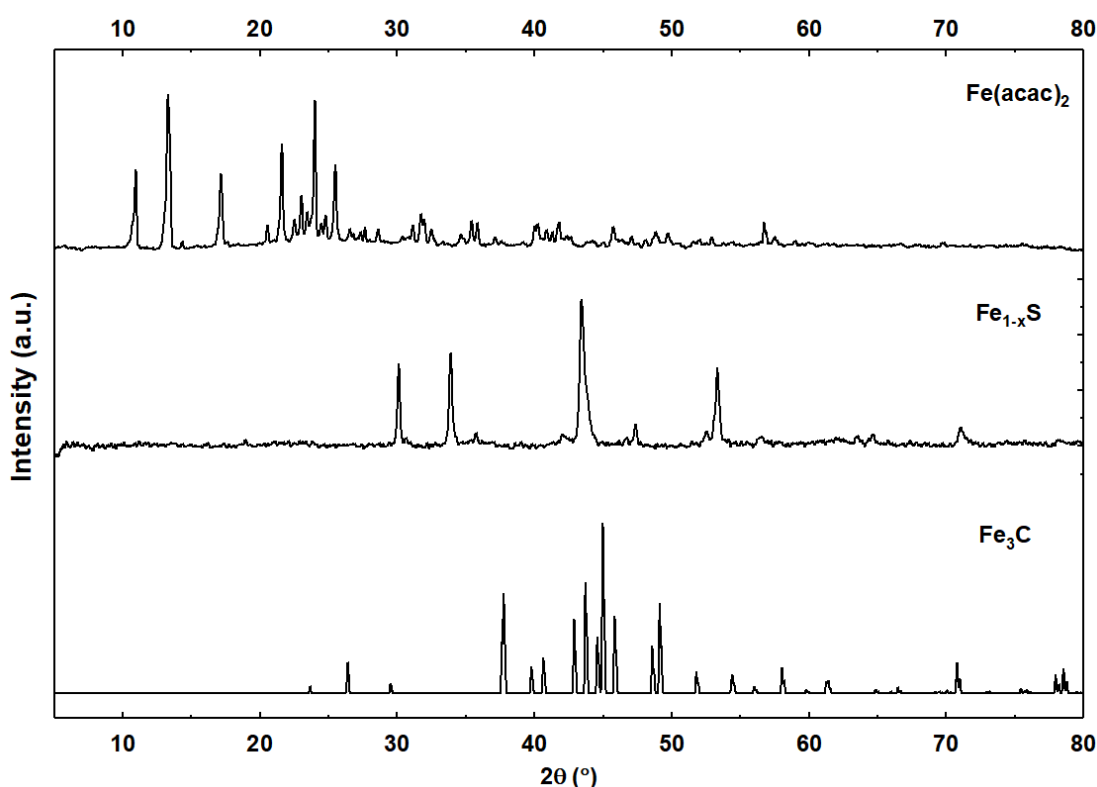


Figure S1: XRD pattern of pyrrhotite (middle) compared to $Fe(acac)_2$ precursor (top) and Fe_3C (bottom) (Fe_3C Sourced from the RRUFF database, R10076).

Table S1: Elemental Analysis of fresh and calcined samples of pyrrhotite.

Sample	Weight %			Atom %			$\text{Fe}_x\text{S}_y\text{O}_z$
	Fe	S	O	Fe	S	O	
Pyrrhotite Fresh	61.62	36.63	1.75	46.8	48.5	4.7	$\text{Fe}_{0.96}\text{SO}_{0.1}$
Pyrrhotite calcined 200 °C	59.35	36.65	4	43.3	46.5	10.2	$\text{Fe}_{0.93}\text{SO}_{0.2}$

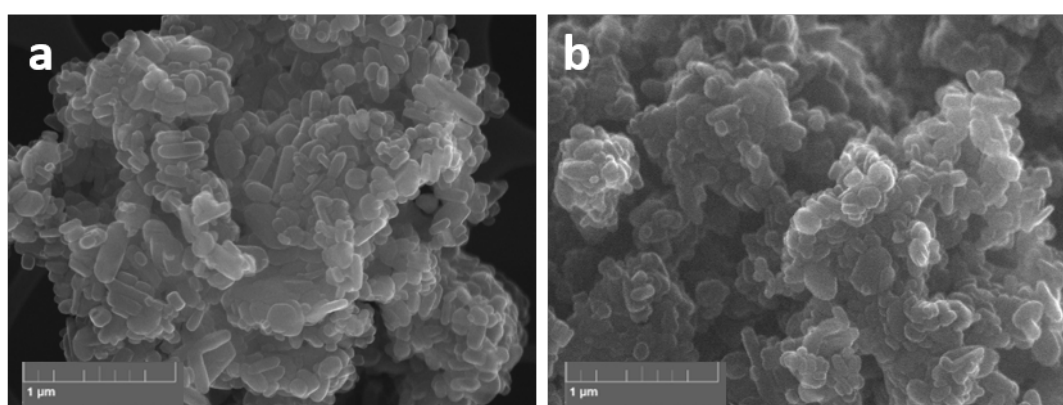


Figure S2: Typical SEM micrographs of (a) fresh pyrrhotite and (b) pyrrhotite calcined at 200 °C. Fresh pyrrhotite shows a surface of clusters of crystallites ranging from 50-450 nm. After calcination, a decrease in crystallite size arises ranging from 40-300 nm.

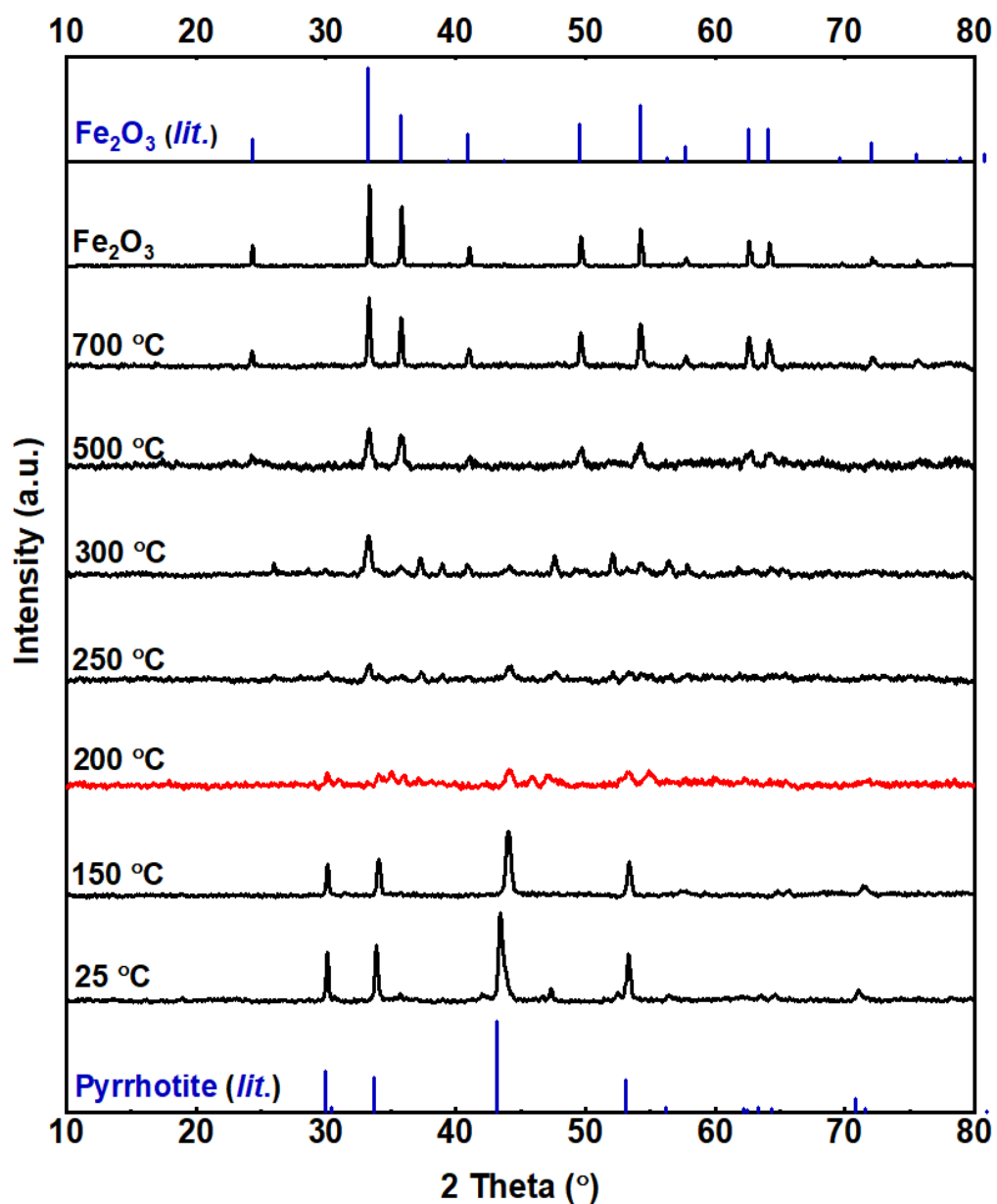


Figure S3: pXRD of pyrrhotite material calcined at different temperatures from fresh – 700 °C. (red)-most catalytically active species, (blue) – Pyrrhotite and Fe_2O_3 reference peaks.

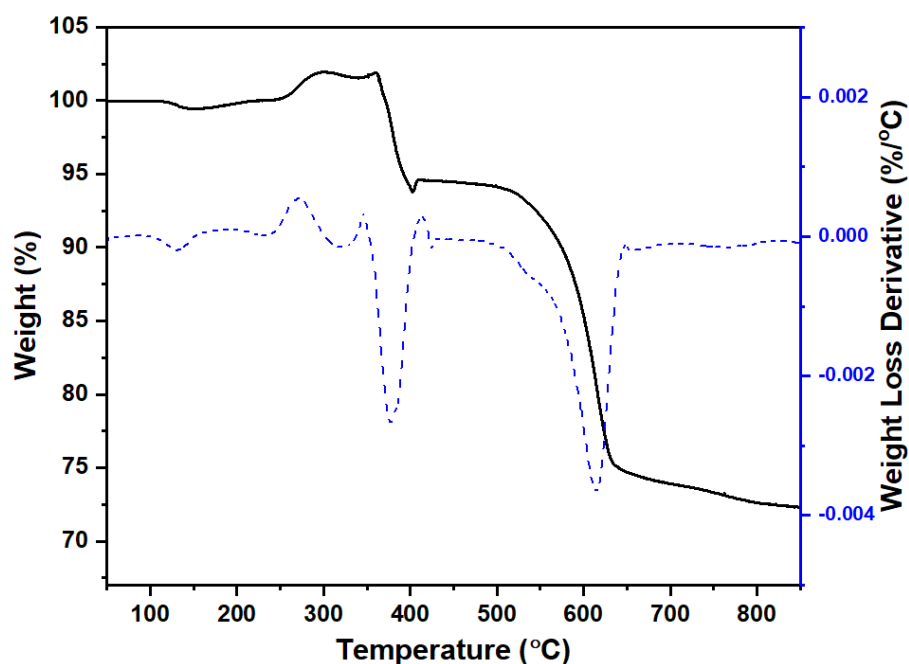


Figure S4: TGA of pyrrhotite heated under air from room temperature to 800 °C, 5°C/min. Percentage weight loss (black) and the first derivative of weight loss (blue). Initial mass loss (at ca. 150 °C) is the result of water and residual toluene evaporation. When increasing the temperature from 150 °C up to 302 °C, the material gained 2.5 % of its original weight from the formation of S-O and Fe-O species. Above 360 °C, a large mass loss (25.1 %) was observed, as sulfoxides are unstable at high temperatures and decompose rapidly with the release of SO₂. From 500 to 640 °C, another large drop in mass of 19.1 % was observed, corresponding to the complete removal of sulfur as SO₂ to form Fe₂O₃.

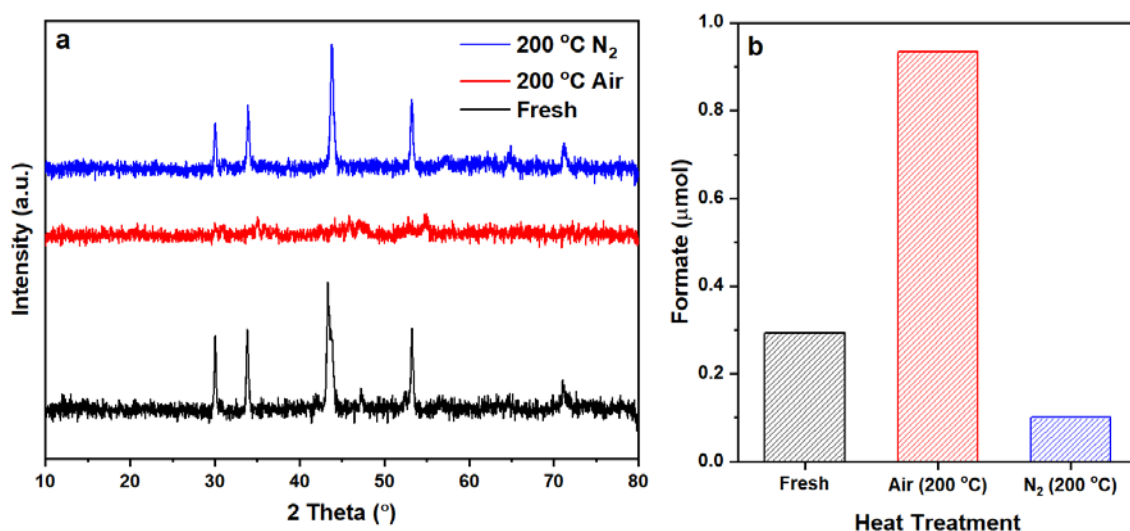


Figure S5:(a) XRD pattern and (b) formate production as a result of different heat treatments. (black) none (red) 200 °C under flowing air (blue) 200 °C under flowing nitrogen. Reaction conditions: catalyst: 20mg; 1M NaOH solution: 4 ml; pCO₂:H₂: (1:1) 20 bar; 125 °C for 3 days.

Table S2: Binding energy data and interpretations for the XPS Fe2p and S2p spectra of fresh and calcined pyrrhotite samples. Peak reference correlating to spectra in Figures 3a-d and S4.

XPS spectra	<i>Fresh</i>			<i>Calcined 200 °C</i>			<i>Calcined 300 °C</i>		
	B.E. (eV)	Chemical state	Atom Conc (%) ($\pm 10\%$)	B.E. (eV)	Chemical state	Atom Conc (%) ($\pm 10\%$)	B.E. (eV)	Chemical state	Atom Conc (%) ($\pm 10\%$)
Fe2p	707.3	Fe(II)-S	25	707.6	Fe(II)-S	3	707.2	Fe(II)-S	2
	710.1	Fe(III)-O	44	710.4	Fe(III)-O	54	710.1	Fe(III)-O	46
	711.6	Fe(III)-O	21	711.8	Fe(III)-O	32	711.5	Fe(III)-O	36
	713.3	Fe(III)-O	10	713.4	Fe(III)-O	11	713.2	Fe(III)-O	16
S2p	161.2	S ²⁻	36	161.3	S ²⁻	4	160.4	S ²⁻	3
	162.4		19	162.5		2	161.6		1
	162.2	S ₂ ²⁻	7	162.6	S ₂ ²⁻	12	162.4	S ₂ ²⁻	18
	163.3		4	163.7		6	163.6		9
	163.2	S _n ²⁻	8	164.1	S _n ²⁻	4	-	S _n ²⁻	-
	164.4		4	165.3		2	-		-
	164.1	S ₈	3	164.8	S ₈	3	165.0	S ₈	3
	165.3		2	166.0		2	166.2		1
	166.6	SO ₃ ²⁻	3	167.5	SO ₃ ²⁻	4	-	SO ₃ ²⁻	-
	167.7		2	168.6		2	-		-
	168.2	SO ₄ ²⁻	8	168.8	SO ₄ ²⁻	39	168.5	SO ₄ ²⁻	43
	169.4		4	169.9		20	169.7		22

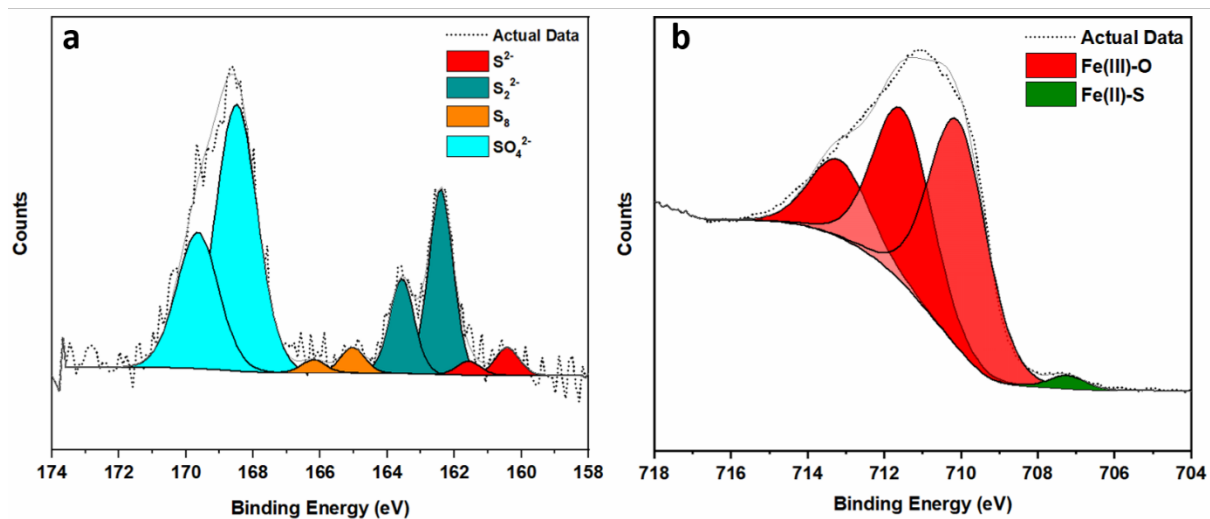


Figure S6: XPS spectra of pyrrhotite calcined at 300 °C (a) Fe2p (b) S2p. Binding energy data listed in Table S2.

Computational Details

Density Functional Theory Calculations

All geometry optimisations were performed with VASP 5.3^{2,3} using the PBE functional⁴ and the same U parameter of 1 eV as in previous works on troilite^{5,6}. We have employed the projector augmented wave method to model the core-electron interaction⁷, treating explicitly the following electrons: Fe 3p 3d 4s; S 3s 3p; O 2s 2p; C 2s 2p; H 1s. The spin configuration of troilite, antiferromagnetic along the c -axis⁸, was used as starting configuration for all surfaces, which were formed of six FeS layers. The optimisations were performed with a plane wave cutoff of 400 eV and a $4 \times 2 \times 1$ Monkhorst-Pack grid, keeping fixed the two bottom layers⁹. Geometry optimisation was stopped when the forces acting on the ions were less than 10^{-2} eV/Å. Surface slabs were separated by a vacuum region of at least 12 Å along the normal direction. Transition states were located with the climbing image nudged elastic band algorithm, using five images¹⁰.

Computational Surface Models

As a model for the catalytic surface, we have used the prismatic (01-10) surface of stoichiometric FeS end-member of the pyrrhotite group¹¹, where we have considered four different terminations (A, B1, B2 and B3; see Figure S7). Termination A (Figure S7a) was obtained by replacing all the sulfur atoms in the top layer of the surface by oxygen atoms, which is justified in view of the considerable amount of oxidation occurring even in the fresh sample, but even more so in the calcined samples. Terminations B1, B2 and B3 are obtained by changing back one of the resulting three inequivalent surface oxygen atoms to a surface sulfur atom, to allow for the remaining surface sulfur species found experimentally in the fresh and calcined samples at 200 °C. After testing the relative stabilities of the three sulfur-containing terminations, we have focussed on the most stable surface, which we henceforth refer to as termination B (Figure S7b).

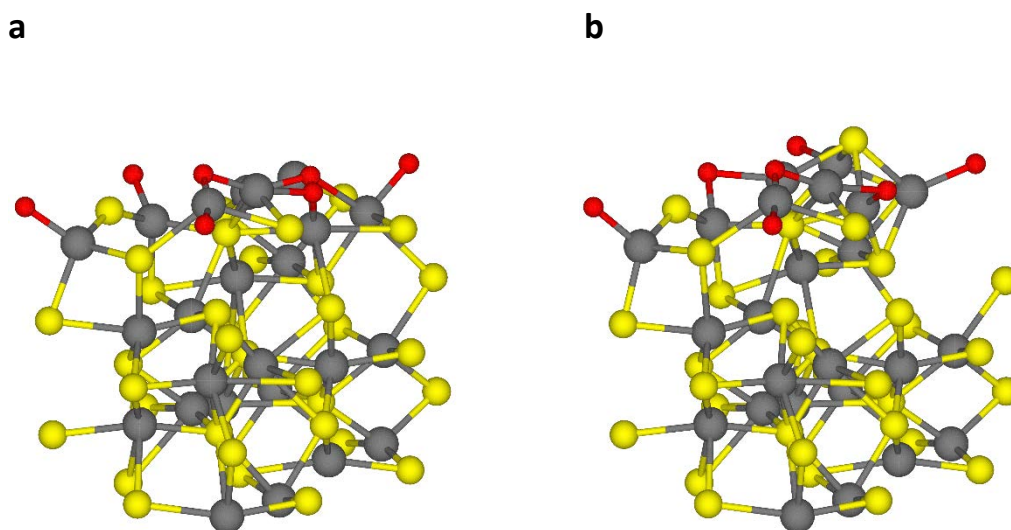


Figure S7: The fully oxidised A (a) and sulfur-containing oxidised B (b) surface terminations. Colour code: Fe-grey, S-yellow, O-red.

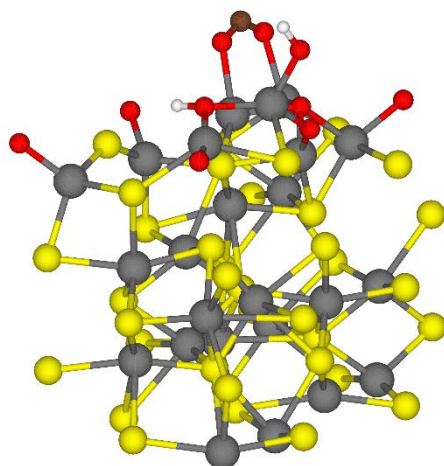


Figure S8: Adsorption of OH^- and CO_2 . A H^+ species is used to neutralise the cell. Colour code: Fe-grey, S-yellow, O-red, C-brown, H-white.

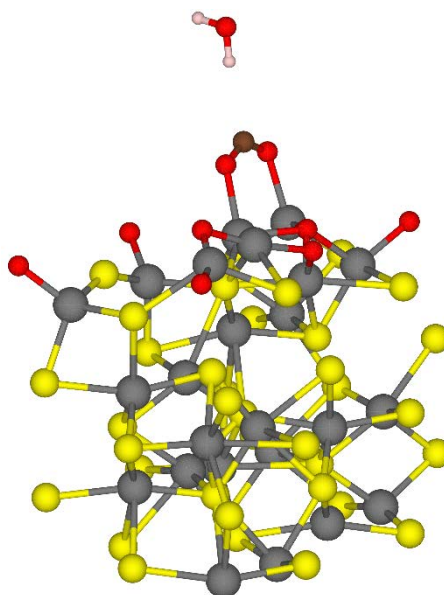


Figure S9: Elimination of a water molecule leaving the bent CO_2 species on the surface. Colour code: Fe-grey, S-yellow, O-red, C-brown, H-white.

References

- 1 J. H. L. Beal, P. G. Etchegoin and R. D. Tilley, *J. Solid State Chem.*, 2012, **189**, 57–62.
- 2 G. Kresse and J. Hafner, *Phys. Rev. B*, 1993, **47**, 558–561.
- 3 G. Kresse and J. Furthmuller, *J. Comput. Mater. Sci*, 1996, **6**, 15–50.
- 4 J. P. Perdew, K. Burke and M. Ernzerhof, *Phys. Rev. Lett*, 1996, **77**, 3865.
- 5 F. Ricci and E. Bousquet, *Phys. Rev. Lett.*, 2016, **116**, 227601.
- 6 U. Terranova and N. H. de Leeuw, *J. Phys. Chem. Solids*, 2017, **111**, 317–323.
- 7 P. E. Blöchl, *Phys. Rev. B*, 1994, **50**, 17953.
- 8 P. Martin, G. D. Price and L. Vočadlo, *Mineral. Mag.*, 2001, **65**, 181–191.
- 9 H. J. Monkhorst and J. D. Pack, *Phys. Rev. B*, 1976, **13**, 5188.
- 10 G. Henkelman, B. P. Uberuaga and H. Jónsson, *J. Chem. Phys.*, 2000, **113**, 9901–9904.
- 11 U. Terranova, C. Mitchell, M. Sankar, D. Morgan and N. H. De Leeuw, *J. Phys. Chem. C*, 2018, **122**, 12810–12818.